

Electronic Supplementary Information

An efficient porous acidic ionic liquid polymer catalyst for Friedel-Crafts acylation reactions

Junhu Zhao, Ming Li, Peng Yang, Xiangyang Jiang, Zhaojin LV, Pier-Luc Tremblay*,
Tian Zhang*

***Correspondence to:** tzhang@whut.edu.cn (T. Zhang), pierluct@whut.edu.cn (P.-L. Tremblay)

Experimental

Chemicals

All reagents were of analytical grade and used without any further treatment. Pluronic P123 (average $M_n = 5800$), Amberlyst 15, and azobisisobutyronitrile (AIBN) were purchased from Sigma-Aldrich (St-Louis, MO, USA). P-Divinylbenzene (p-DVB), *n*-vinylimidazole (VIm), 1,3-propanesultone (Pros), toluene, anisole, tetrahydrofuran (THF), trifluoromethanesulfonic acid/trifluoromethanesulfonate (TfOH/TfO), ether, and sodium *p*-styrenesulfonate hydrate (SPSS) were obtained from Annaiji chemical reagent (Shanghai, China). Acetic anhydride, methanol, anhydrous ethanol, tetraethyl orthosilicate (TEOS), sulfuric acid, dichloromethane, 1,2-dimethoxybenzene, *m*-dimethoxybenzene, *p*-dimethoxybenzene, β -methoxynaphthalene, nitrobenzene, bromobenzene, *m*-xylene, 1,3,5-trimethylbenzene, furan, thiophene, propionic anhydride, butyric anhydride, benzoic anhydride, 1,2-dichloroethane, and aluminum sulfate octadecahydrate were supplied by Sinopharm (Shanghai, China).

Synthesis of the porous ionic liquid polymer solid acid catalyst

The porous ionic liquid (IL) polymer solid acid was synthesized as previously described with several modifications.^{1,2} First, p-DVB was crosslinked with VIm to form the polymer P(DVB-VIm)-*x* where *x* stands for the amount in grams of VIm in the reaction. 2.0 g p-DVB and 0.2, 0.5, or 1.0 g VIm were dissolved in 25 mL THF. Next, 0.8 g AIBN was added to the reaction followed by stirring at 1000 rpm for 2.5 h at room temperature. The mixture was transferred to a Teflon-lined autoclave and incubated at 120 °C for 48 h. After volatilization of the solvent, a fluffy solid was obtained corresponding to P(DVB-VIm)-*x*.

In the next step, P(DVB-VIm)-*x* was modified with Pros. 1.0 g P(DVB-VIm)-*x* was added to 45 mL toluene with 0.8 g Pros in a round-bottom flask followed by stirring at 1000 rpm for 30 min at room temperature. The flask was then connected to a reflux condenser and transferred to an oil bath at 110°C for 24 h. Subsequently, the reaction was cooled down to room temperature and filtrated with a 101 qualitative cellulose

filter paper (Beimu, Hangzhou, China). The collected solid was then washed four times with anhydrous ethanol before being dried in a vacuum oven at 80 °C for 24 h. The resulting material was labeled P(DVB-Vim-Pros)-x.

In the final step of the porous IL polymer solid acid synthesis, P(DVB-Vim-Pros)-x was functionalized with TfOH. 2.0 g P(DVB-Vim-Pros)-x and 20 ml TfOH were both added to 45 mL dichloromethane and stirred at 1000 rpm for 24 h at room temperature. The resulting precipitate was washed 8 times with a mixture made of anhydrous ethanol and dichloromethane (7:3, v:v). After centrifugation at $7100 \times g$ for 10 min at room temperature, the solid was dried in a vacuum oven at 80 °C for 10 h.

Synthesis of PDSH-m and Al-SBA-15

For performance comparison, two other solid acid catalysts described in the literature were synthesized according to previously reported methods.^{3,4} PDSH-m is a copolymer made of DVB and SPSS ion-exchanged with sulfuric acid. For this catalyst, m stands for the content in sulfonic groups. Al-SBA-15-n is made of aluminum incorporated in mesoporous silica (SBA-15). The n value stands for the Si/Al molar ratio. The synthesis process of Al-SBA-15-n required pluronic P123, TEOS, and aluminum sulfate octadecahydrate.

Characterization

X-ray diffraction (XRD) analyses were performed with a D8 Advance diffractometer with a Cu radiation source (Bruker, MA, USA). The N₂ adsorption-desorption isotherms at 77 K were measured with an ASAP 2020 apparatus (Micromeritics, Norcross, GA, USA). The samples were degassed for 12 h at 150 °C before the measurements. Transmission electron microscopy (TEM) experiments were done with a JEM-2100F field emission electron microscope (JEOL, Tokyo, Japan) at an accelerating voltage of 200 kV. For TEM, the samples were first dispersed in ethanol, deposited onto a copper grid, and irradiated with an infrared lamp for 2 hours until being dried. The material's morphology was also studied with a S-4800 field emission

scanning electron microscope (SEM) (Hitachi, Tokyo, Japan) at an accelerating voltage of 15 kV. Fourier transform infrared (FTIR) spectroscopy was performed with a Nicolet 6700 spectrometer (Thermo Fisher Scientific, Waltham, MA, USA) in the 4000 to 400 cm^{-1} range. The acidic site composition of the heterogeneous catalyst was investigated via pyridine adsorption at 120 °C followed by FTIR spectroscopy with a Tensor 27 spectrometer (Bruker). The ^{13}C solid-state cross-polarization magic-angle-spinning nuclear magnetic resonance (CP/MAS NMR) experiment was carried out with an AVANCE NEO 400WB spectrometer (Bruker). The thermogravimetric (TG) analysis was done with a TGA/DSC 2 analyzer (Mettler-Toledo, Columbus, OH, USA) in flowing air with a heating rate of 20°C/min.

Acid-based titration

The acid capacity of the different catalysts was determined by acid-base titration.^{5,6} Briefly, 0.1 g of solid catalyst was suspended in 10 ml methanol. 25 ml of a saturated NaCl solution was then added followed by stirring at 600 rpm for 48 h at room temperature. After filtration, the filtrate was treated with 0.1 M NaOH in the presence of a phenolphthalein indicator.

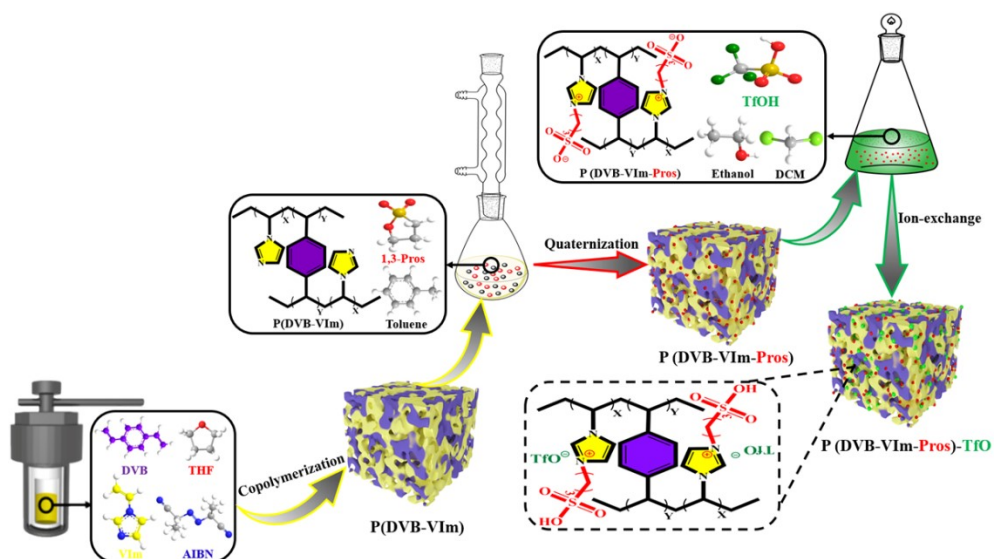
Evaluation of the acylating performance of catalysts

The performance evaluation of the catalysts was carried out in a round bottom flask equipped with a reflux condenser. To maintain a constant reaction temperature, an oil bath with a magnetic stirrer was employed. After optimizing the reaction conditions, a typical experiment with P(DVB-VIm-Pros)-TfO consisted in adding 0.1 mol anisole and 0.3 mol acetic anhydride to 35 ml dichloromethane in a 50 ml three-neck flask. Next, 0.6 g catalyst was added and the reaction was conducted at 120°C for 12 h under stirring at 1000 rpm. Where indicated, other aryl ether substrates and acid anhydride acylating agents were employed. After the reaction, the mixture was cooled down to room temperature and the catalyst was recuperated by centrifugation at $10000 \times g$ for 10 min at room temperature. For the recycling experiment, the catalyst was washed 4 times with ether and then dried in a vacuum oven at 80 °C for 6 h between each round

of acylation.

Gas chromatography

For the analysis of the FCA reagents and products, a GC 9720 gas chromatograph equipped with a RB-1 non-polar column and a FID detector was employed. In a typical experiment with acetic anhydride and anisole, the carrier gas was high-purity N₂ at a flow rate of 50 ml/min. The sample injection volume was 1 µl, the initial temperature was kept at 120 °C for 1 min, then it was raised to 280 °C at a 10 °C/min rate. For other FCA reactions with different acylating agents and substrates, the gas chromatography parameters were changed with column temperatures ranging from 150 to 360 °C and rates of 10-20 °C.



Scheme S1. The synthesis route of P(DVB-VIm-Pros)-TfO. In the first step, p-DVB was copolymerized with VIm to form P(DVB-VIm). Next, the IL polymer was modified with Pros by quaternization. In the last step, P(DVB-VIm-Pros) was functionalized with TfO via ion exchange.

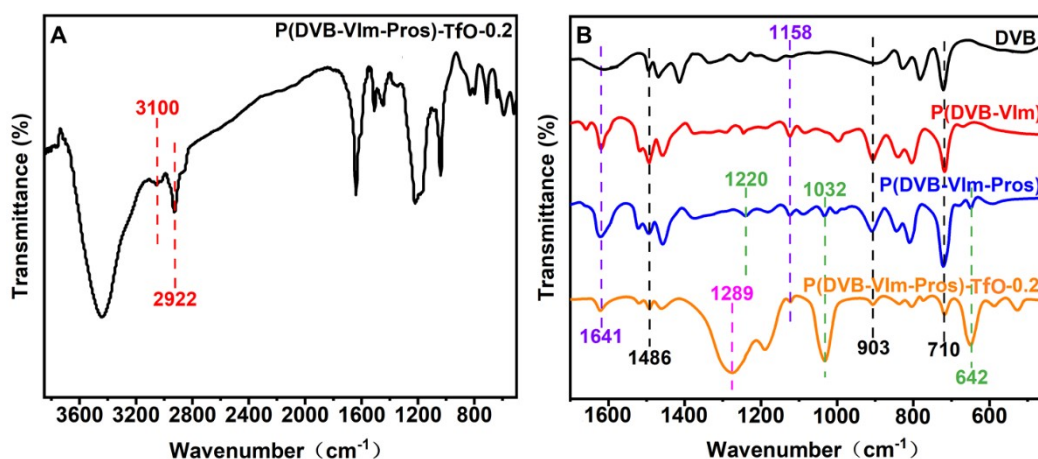


Fig.S1. (A) The full FTIR spectrum of P(DVB-VIm-Pros)-TfO-0.2. (B) FTIR spectra from 1700 cm^{-1} to 450 cm^{-1} for DVB, P(DVB-VIm), P(DVB-VIm-Pros), and P(DVB-VIm-Pros)- TfO-0.2.

FTIR spectroscopy was conducted to confirm the successful synthesis of the porous IL polymer solid acid P(DVB-VIm-Pros)-TfO (Fig. S1). The final polymer as well as all the controls from the different stages of the synthesis process displayed bands distinctive of the benzene rings found in DVB including -CH (903 cm^{-1} , 1486 cm^{-1} , and 3100 cm^{-1}), $-\text{CH}_2$ (2922 cm^{-1}), and C-C (710 cm^{-1}) functional groups.⁷ After the polymerization of DVB and VIm, P(DVB-VIm), P(DVB-VIm-Pros), and P(DVB-VIm-Pros)-TfO-0.2 exhibited FTIR bands at 1641 cm^{-1} and 1158 cm^{-1} corresponding to C-N stretching vibrations from the amino-alkyl chain of the imidazole group.^{8,9} The spectrum of P(DVB-VIm-Pros) also included bands at 642 cm^{-1} , 1032 cm^{-1} , and 1220 cm^{-1} assigned to S-O, C-S, and C=S, demonstrating the effective quaternization of the polymer with Pros.^{7,10} Two of these peaks (642 cm^{-1} and 1032 cm^{-1}) were detected on the spectrum of the final P(DVB-VIm-Pros)-TfO-0.2 material, but the peak at 1220 cm^{-1} was not apparent because it overlapped with a wide band at 1289 cm^{-1} characteristic of the C-F group in TfO. Another evidence of the TfO grafting on P(DVB-VIm-Pros) was the increased intensities of the peaks corresponding to S-O (642 cm^{-1}) and C-S (1220 cm^{-1}), which was due to the higher sulfur content.^{2,11}

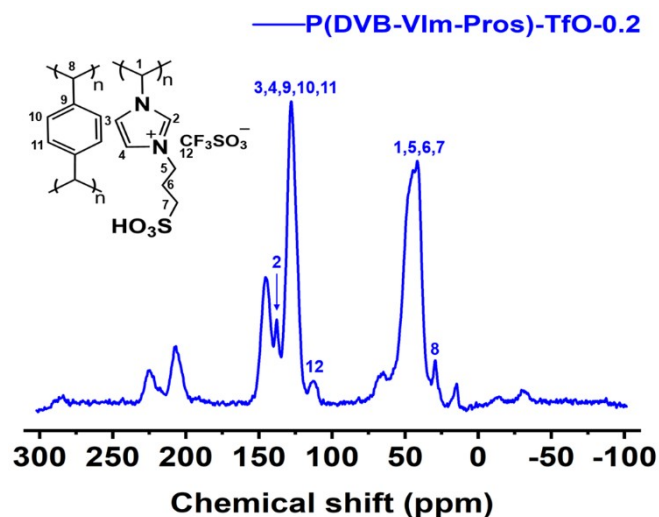


Fig. S2. Solid-state ^{13}C NMR spectrum of P(DVB-VIm-Pros)-TfO-0.2.

The polymeric framework of P(DVB-VIm-Pros)-TfO-0.2 was investigated further by solid-state ^{13}C CP/MAS NMR (Fig. S2). The ^{13}C NMR spectrum of P(DVB-VIm-Pros)-TfO-0.2 displayed a sharp overlapping peak at 128 ppm, corresponding to the C3 and C4 atoms in the imidazolium ring and the C9, C10, and C11 carbons of the benzene ring. The chemical shift peak at 138 ppm can be attributed to the C2 atom in the imidazolium ring.¹² The group of peaks (5, 6, and 7) at ca. 42 ppm was ascribed to the carbon side chain connecting SO_3H to the cationic imidazolium ring.¹³ The peak generated by the C12 atom of TfO was detected at ca. 120 ppm.¹⁴ In addition, two peaks at 29 (8) and 42 ppm (1) corresponded to aliphatic bridge chains.¹³ Thus, solid-state ^{13}C CP/MAS NMR results provide supplementary evidence of the correct structure of P(DVB-VIm-Pros)-TfO-0.2.

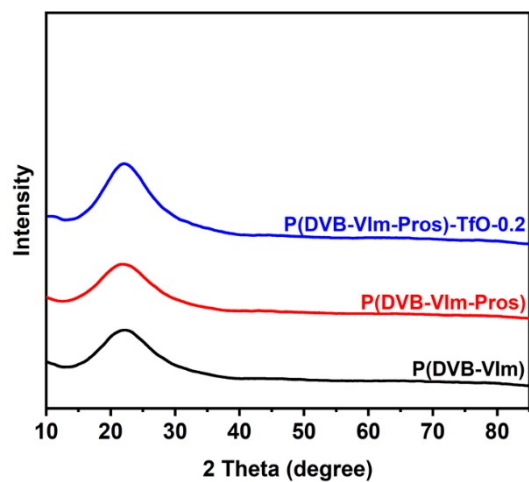


Fig. S3. XRD spectra of P(DVB-VIm), P(DVB-VIm-Pros), and P(DVB-VIm-Pros)-TfO-0.2.

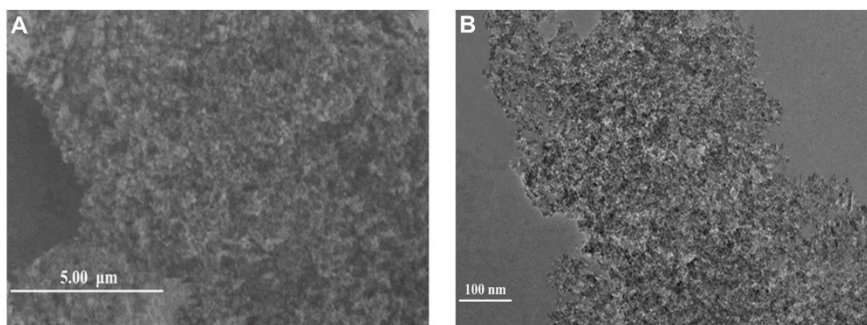


Fig. S4. (A) SEM and (B) TEM micrographs of P(DVB-VIm-Pros)-TfO-0.2.

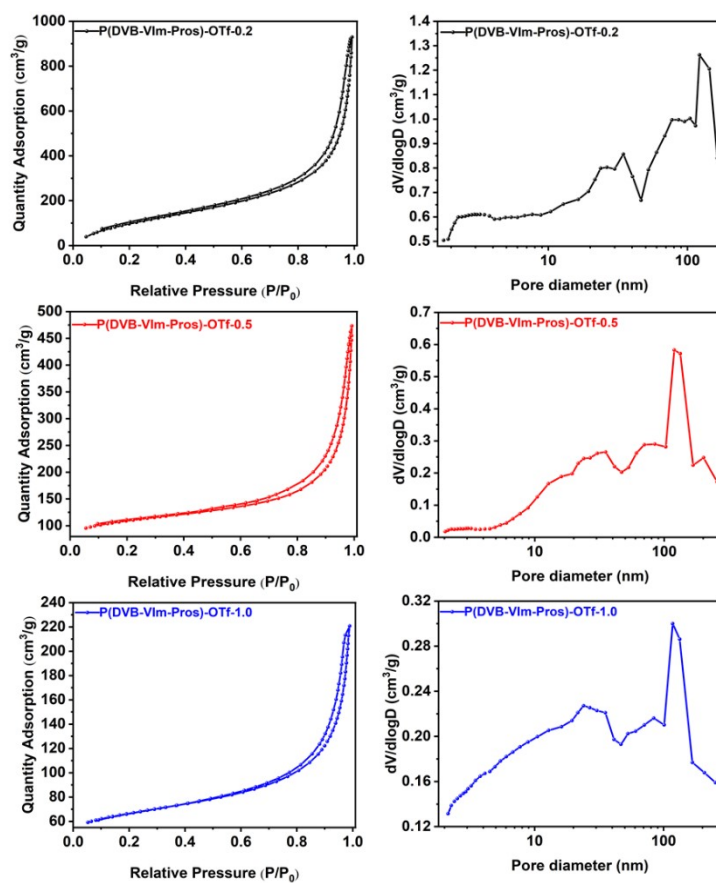


Fig. S5. N_2 adsorption-desorption isotherms and pore distribution curves of P(DVB-VIm-Pros)-TfO-0.2, P(DVB-VIm-Pros)-TfO-0.5, and P(DVB-VIm-Pros)-TfO-1.0.

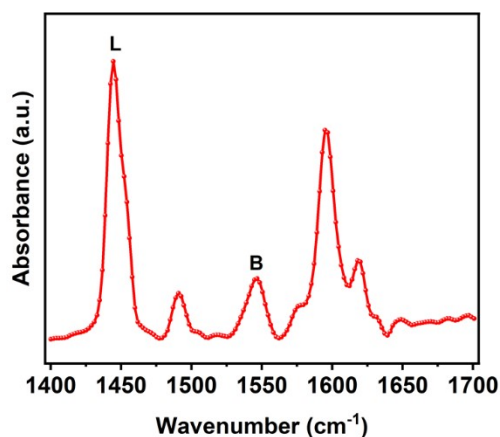


Fig. S6. FTIR spectrum of P(DVB-VIm-Pros)-TfO-0.2 after pyridine adsorption at 120 °C.

A pyridine adsorption experiment at 120 °C followed by a FTIR analysis indicated that Lewis acidic sites were more abundant in P(DVB-VIm-Pros)-TfO-0.2 than Brønsted acidic sites in a 3.27 to 1 ratio (Fig. S6). The FTIR spectrum displayed typical bands associated with pyridine bound to Lewis (L) and Brønsted (B) acidic sites at 1450 cm^{-1} and 1540 cm^{-1} , respectively.¹⁵ In addition, a peak at 1490 cm^{-1} distinctive of pyridine bound simultaneously to Brønsted and Lewis acidic sites and a peak at 1598 cm^{-1} characteristic of hydrogen-bound pyridine were observed.

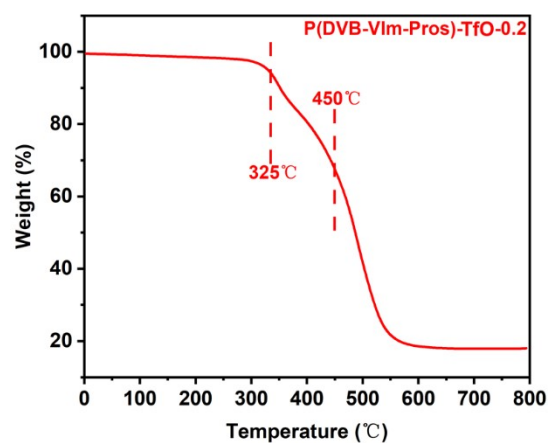


Fig. S7. The TG curve of P(DVB-VIm-Pros)-TfO-0.2. The TG experiment was performed in air with a heating rate of 20°C/min.

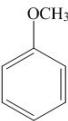
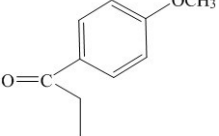
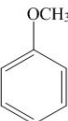
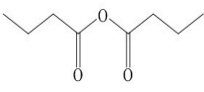
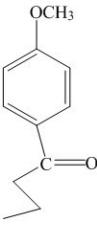
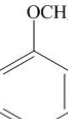
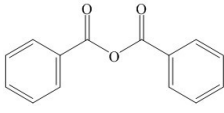
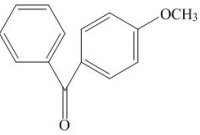
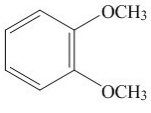
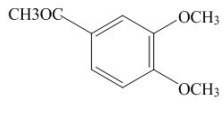
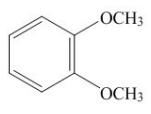
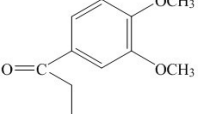
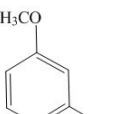
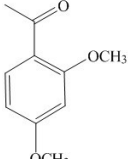
Table S1. Surface and acidic properties of the solid acid catalysts.


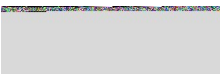
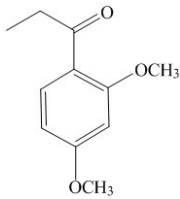


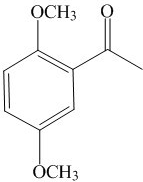

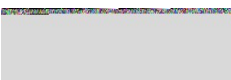
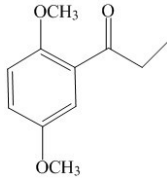
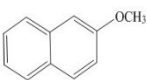

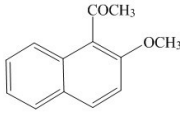
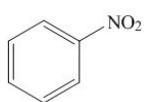
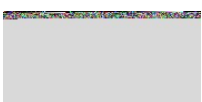
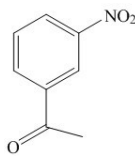
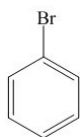

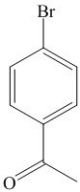
Catalyst	Acid capacity^a (mmol/g)	SSA^b (m²/g)	V_p^c (cm³/g)	D_p^d (nm)
P(DVB-VIm-Pros)-0.2	0.44	780	1.54	22.5
P(DVB-VIm-Pros)-TfO-0.2	1.23	587	1.36	29.5
P(DVB-VIm-Pros)-TfO-0.5	2.36	264	0.74	25.8
P(DVB-VIm-Pros)-TfO-1.0	4.15	78	0.21	19.4
PDSH-1	0.58	498	0.94	11.5
PDSH-5	1.74	283	0.32	6.8
Al-SBA-15-5	1.06	636	1.10	7.3
Al-SBA-15-10	1.82	443	1.06	8.4
Amberlyst 15	4.68	50	0.40	40

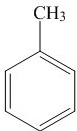
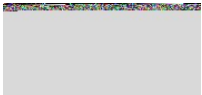
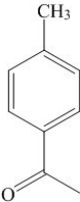
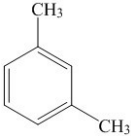

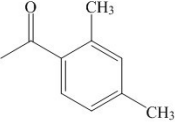
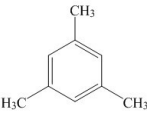
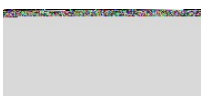
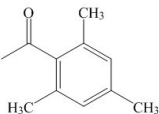

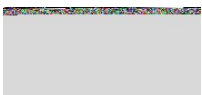
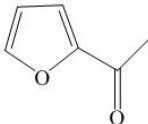


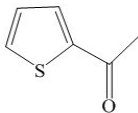
^aThe acid capacity was measured by acid-base titration. ^bSSA: specific surface area.

^cV_p: total pore volume. ^dD_p: average pore diameter.

Table S2. Acylation reactions catalyzed by P(DVB-VIm-Pros)-TfO-0.2 with different substrates and acylating agents.^a

Entry	Substrate	Acylating agent	Conversion (%)	Target product	Selectivity (%)
1	 Anisole	$\text{H}_3\text{C}-\text{CH}_2-\overset{\text{O}}{\parallel}{\text{C}}-\text{O}-\overset{\text{O}}{\parallel}{\text{C}}-\text{CH}_2-\text{CH}_3$ Propionic anhydride	85.2	 4-Methoxypropiofenone	92.8
2	 Anisole	 Butyric anhydride	82.6	 4-Methoxyphenbutanone	91.3
3	 Anisole	 Benzoic anhydride	73.4	 4-Methoxybenzophenone	88.7
4	 1,2-Dimethoxybenzene	$\text{H}_3\text{C}-\overset{\text{O}}{\parallel}{\text{C}}-\text{O}-\overset{\text{O}}{\parallel}{\text{C}}-\text{CH}_3$ Acetic anhydride	70.8	 3,4-Dimethoxyacetophenone	92.4
5	 1,2-Dimethoxybenzene	$\text{H}_3\text{C}-\text{CH}_2-\overset{\text{O}}{\parallel}{\text{C}}-\text{O}-\overset{\text{O}}{\parallel}{\text{C}}-\text{CH}_2-\text{CH}_3$ Propionic anhydride	65.2	 3,4-Dimethoxypropiofenone	92.7
6	 <i>m</i> -Dimethoxybenzene	$\text{H}_3\text{C}-\overset{\text{O}}{\parallel}{\text{C}}-\text{O}-\overset{\text{O}}{\parallel}{\text{C}}-\text{CH}_3$ Acetic anhydride	63.6	 2,4-Dimethoxyacetophenone	93.2

7	 <p><i>m</i>-Dimethoxybenzene</p>	 <p>Propionic anhydride</p>	61.3	 <p>2,4-Dimethoxypropiophenone</p>	92.6
8	 <p><i>p</i>-Dimethoxybenzene</p>	 <p>Acetic anhydride</p>	56.8	 <p>2,5-Dimethoxyacetophenone</p>	93.4
9	 <p><i>p</i>-Dimethoxybenzene</p>	 <p>Propionic anhydride</p>	50.5	 <p>2,5-Dimethoxypropiophenone</p>	92.4
10	 <p>β-Methoxynaphthalene</p>	 <p>Acetic anhydride</p>	40.2	 <p>β-Methoxynaphthyl ethyl ketone</p>	91.3
11	 <p>Nitrobenzene</p>	 <p>Acetic anhydride</p>	26.8	 <p>3-Nitroacetophenone</p>	58.4
12	 <p>Bromobenzene</p>	 <p>Acetic anhydride</p>	34.3	 <p>4-Bromoacetophenone</p>	67.2

13	 Toluene	 Acetic anhydride	58.4	 4-methylacetophenone	65.3
14	 m-Xylene	 Acetic anhydride	69.8	 2,4-Dimethylacetophenone	78.2
15	 (1,3,5-Trimethylbenzene)	 Acetic anhydride	81.2	 2,4,6-Trimethylacetophenone	89.6
16	 Furan	 Acetic anhydride	69.4	 2-Acetylfuran	83.7
17	 Thiophene	 Acetic anhydride	78.3	 2-Acetylthiophene	81.5

^aReaction conditions: substrate (3 mmol), acylating agent (9 mmol), 0.6 g of catalyst, 35 ml 1,2-dichloroethane, 120 °C, 12 h, agitation speed of 1000 rpm.

References

- 1 F. Liu, R. K. Kamat, I. Noshadi, D. Peck, R. S. Parnas, A. Zheng, C. Qi and Y. Lin, *Chem. Commun.*, 2013, **49**, 8456–8458.
- 2 D. Yuan, L. Li, F. Li, Y. Wang, F. Wang, N. Zhao and F. Xiao, *ChemSusChem*, 2019, **12**, 4986–4995.
- 3 D. Yuan, N. Zhao, Y. Wang, K. Xuan, F. Li, Y. Pu, F. Wang, L. Li and F. Xiao, *Appl. Catal. B Environ.*, 2019, **240**, 182–192.
- 4 S. Wu, Y. Han, Y.-C. Zou, J.-W. Song, L. Zhao, Y. Di, S.-Z. Liu and F.-S. Xiao, *Chem. Mater.*, 2004, **16**, 486–492.
- 5 S. Zhu, J. Xu, Z. Cheng, Y. Kuang, Q. Wu, B. Wang, W. Gao, J. Zeng, J. Li and K. Chen, *Appl. Catal. B Environ.*, 2020, **268**, 118732.
- 6 C. Miranda, A. Ramírez, A. Sachse, Y. Pouilloux, J. Urresta and L. Pinard, *Appl. Catal. A Gen.*, 2019, **580**, 167–177.
- 7 K.-S. Lin, N. V. Mdlovu, H.-Y. Chan, K. C.-W. Wu, J. C.-S. Wu and Y.-T. Huang, *Catal. Today*, 2022, **397–399**, 145–154.
- 8 X. Song, Y. Wu, D. Pan, J. Zhang, S. Xu, L. Gao, R. Wei and G. Xiao, *J. CO₂ Util.*, 2018, **28**, 326–334.
- 9 Z. Guo, X. Cai, J. Xie, X. Wang, Y. Zhou and J. Wang, *ACS Appl. Mater. Interfaces*, 2016, **8**, 12812–12821.
- 10 J. Scaranto, A. P. Charnet and S. Giorgianni, *J. Phys. Chem. C*, 2008, **112**, 9443–9447.
- 11 N. Wei, Y. Zhang, H. Zhang, T. Chen and G. Wang, *React. Funct. Polym.*, 2022, **171**, 105156.
- 12 Y. He, X. Li, W. Cai, H. Lu, J. Ding, H. Li, H. Wan and G. Guan, *ACS Sustain. Chem. Eng.*, 2021, **9**, 7074–7085.
- 13 Z. Guo, Q. Jiang, Y. Shi, J. Li, X. Yang, W. Hou, Y. Zhou and J. Wang, *ACS Catal.*, 2017, **7**, 6770–6780.
- 14 P. Stiernet, M. Mazaj, S. Kovačič and A. Debuigne, *Chem. Eng. J.*, 2022, **446**, 137012.
- 15 A. Martins, V. Neves, J. Moutinho, N. Nunes and A. P. Carvalho, *Microporous*

Mesoporous Mater., 2021, **323**, 111167.